

Effects of CD4⁺ T lymphocytes from ovariectomized mice on bone marrow mesenchymal stem cell proliferation and osteogenic differentiation

BING-YI SHAO¹⁻³, LAN WANG¹⁻³, YANG YU¹⁻³, LIANG CHEN¹⁻³,
NING GAN¹⁻³ and WEN-MING HUANG¹⁻³

¹Department of Operative Dentistry and Endodontics; ²Chongqing Key Laboratory of Oral Diseases and Biomedical Sciences; ³Chongqing Municipal Key Laboratory of Oral Biomedical Engineering of Higher Education, Stomatological Hospital of Chongqing Medical University, Chongqing 400047, P.R. China

Received May 31, 2019; Accepted May 28, 2020

DOI: 10.3892/etm.2020.9212

Abstract. The present study was designed to investigate the effects of T cells on the proliferation and osteogenic differentiation of bone marrow mesenchymal stem cells (BMMSCs). BMMSCs were co-cultured with CD4⁺ T cells that had been pretreated with anti-TNF- α or controls and were derived from ovariectomized (OVX) mice or sham control mice. MTT was used to assess the proliferative ability of BMMSCs and flow cytometry was used to analyze the BMMSC cell cycle. Following the induction of osteogenic differentiation in BMMSCs, calcium nodules were observed using alizarin red staining and alkaline phosphatase (ALP) staining. The expression levels of the osteogenesis-associated genes, runt related transcription factor 2 (Runx2) and osteocalcin (OCN) in BMMSCs were quantified using reverse transcription-quantitative PCR and western blotting. Osteogenesis-related signaling pathways, including ERK, JNK and p38 MAPK were also examined by western blotting. BMMSCs co-cultured with CD4⁺ T cells from OVX mice exhibited reduced proliferative ability compared with sham mice and the cell cycle was arrested at the G2/M phase. Additionally, BMMSCs co-cultured with CD4⁺ T cells from OVX mice presented with reduced levels of osteogenic differentiation and lower ALP activity, less calcium deposition and reduced expression of Runx2 and OCN compared with sham mice. The reduced levels of proliferation and osteogenic differentiation of BMMSCs induced by CD4⁺ T cells were not seen when the T cells were had been pretreated with anti-TNF- α . The

results indicated that CD4⁺ T cells from OVX mice inhibited the proliferation and osteogenic differentiation of BMMSCs by producing high levels of TNF- α and may provide a novel insight into the dysfunction of BMMSCs caused by estrogen deficiency.

Introduction

Osteoporosis is a metabolic disease of the bones characterized by low bone mass and the micro-architectural deterioration of bone tissue (1). This disease causes bones to break more easily in affected individuals compared with normal, healthy patients. Osteoporosis is particularly common in older women (2). In 2017, it was estimated that >200 million people worldwide suffer from osteoporosis (3). In the USA, ~50% of all postmenopausal women had osteoporosis in 2018 (4). Postmenopausal osteoporosis (PMO) occurs as a result of decreased estrogen levels and increased bone immune function, resulting in an imbalance in bone remodeling (5). Estrogen is a well-known regulator of the immune system and T-cell function (6) and regulates T cell activation via the classical estrogen receptor pathway (7). As it is currently understood, T cells serve a pivotal role in the pathogenesis of PMO (8). In ovariectomized (OVX) mice, an animal model of PMO, increased proliferation of activated T cells has been observed (9). Furthermore, several subsets of T cells, including CD4⁺ T cells, have been demonstrated to be present at increased levels in the peripheral blood of patients with osteoporosis (10). In a study where bone loss was induced in nude mice via ovariectomy, levels were subsequently restored by transferring wild-type T cells into the mice (8). Additionally, depletion of T cells can be counteracted anti-CD4/CD8 antibody treatment, which protects OVX mice from ovariectomy-associated bone loss (11). Recently, Song *et al* (12) discovered that vascular endothelial cells secrete exosomes that attenuate bone loss via microRNA-155 in OVX mice. Additional studies have reported that estrogen reduction promoted the proliferation of T cells and that activated T cells expressed high levels of pro-osteoclastogenic cytokines, TNF- α and receptor activator

Correspondence to: Dr Wen-Ming Huang, Department of Operative Dentistry and Endodontics, Stomatological Hospital of Chongqing Medical University, 426 Songshibeilu Street, Chongqing 400047, P.R. China
E-mail: 500624@hospital.cqmu.edu.cn

Key words: osteoporosis, T cells, bone marrow mesenchymal stem cells, osteogenesis, TNF- α

of the NF- κ B ligand (13-15), which promote the activation of osteoclasts and break the dynamic balance of bones (16,17). These findings indicated that the activation of T cells promotes osteoclastogenesis.

Mesenchymal stem cells (MSCs) are ideal multipotent stem cells for tissue regeneration due to their excellent capacities for proliferation and differentiation. After differentiation is induced *in vitro* or *in vivo*, MSCs can differentiate into several types of tissues, including fat, muscle, bone, cartilage, tendon, ligament, nerve and liver tissue (18-20). As a type of MSC, bone marrow mesenchymal stem cells (BMMSCs) are widely used in studies of bone regeneration due to their properties of multipotency and active proliferation (21). BMMSCs are a class of adult stem cells present in the bone marrow stroma and participate in the formation of the bone marrow microenvironment. Furthermore, BMMSCs have the potential to differentiate into mesoderm and neuroectoderm-derived tissue cells (22). Functional defects, including decreased proliferative activity and decreased osteogenic differentiation of BMMSCs, lead to the onset of PMO (23).

Current research is largely focused on the interaction between T cells and osteoblasts and osteoclasts (24), while there are few reports on the effects of T cells on the proliferation and differentiation of BMMSCs (25,26). In the present study, an osteoporosis model was established in order to elucidate the effects of T cells on the proliferation and differentiation of BMMSCs and to further explore the pathogenesis of PMO.

Materials and methods

Reagents and chemicals. A variety of reagents and chemicals were used in the current study, including: α -minimum essential medium (MEM; Gibco; Thermo Fisher Scientific, Inc.), trypsin (Gibco; Thermo Fisher Scientific, Inc.), FBS (Tianhang; Zhejiang Tianhang Biotechnology Co., Ltd.), phenol red-free α -MEM (Gibco; Thermo Fisher Scientific, Inc.), RPMI-1640 medium (Gibco; Thermo Fisher Scientific, Inc.), a total RNA extraction kit (Takara Bio, Inc.), a one-step reverse transcription-PCR kit (Takara Bio, Inc.) and magnetic beads coated with anti-mouse CD4 antibodies (Miltenyi Biotec., Inc.), CD3 and CD28 (both, BD Biosciences), a volumetric microscope, an inverted phase contrast microscope and camera system (Olympus Corporation), a flow cytometer (Beckman Coulter, Inc.), an Alkaline Phosphatase Staining kit (cat. no. P0321; Beyotime Institute of Biotechnology), a mouse TNF- α ELISA kit (cat. no. MTA00B; R&D Systems, Inc.), anti-TNF- α antibodies (cat. no. AF-410-NA; R&D Systems, Inc.), FITC-conjugated anti-CD3 (cat. no. 11-0032-82; eBioscience; Thermo Fisher Scientific, Inc.), allophycocyanin (APC)-conjugated anti-CD4 (cat. no. 17-0042-82; eBioscience; Thermo Fisher Scientific, Inc.), phycoerythrin (PE)-conjugated anti-CD69 (cat. no. 12-0691-82; eBioscience; Thermo Fisher Scientific, Inc.) and Armenian hamster IgG isotype control (cat. no. 12-4888-81; eBioscience; Thermo Fisher Scientific, Inc.). Furthermore, anti-runt related transcription factor 2 (Runx2; cat. no. ab76956), anti-osteocalcin (OCN; cat. no. ab93876), anti-p-ERK (cat. no. ab217322), anti-ERK (cat. no. ab17942), anti-p-JNK (cat. no. ab4821), anti-JNK

(cat. no. ab112501), anti-p-P38 (cat. no. ab47363), anti-P38 (cat. no. ab197348) and anti- β -actin (cat. no. ab8227) were purchased from Abcam and used for the current research.

PMO mouse model. Animal studies were reviewed and approved by the Animal Care and Use Committee of Chongqing Medical University (Chongqing, China; approval no. 2018101702) and carried out according to their guidelines. A total of 30 female C57BL/6 mice (age, 6-8 weeks; weight, 21-25 g) were housed in a room at a humidity of 50 \pm 10% and a controlled temperature of 25 \pm 1 $^{\circ}$ C with 12-h light/dark cycles. The mice were maintained in an individually ventilated cage system and provided with free access to sterile food and water. The mice were randomly divided into either the OVX group (n=15) or the sham group (n=15). Mice were anesthetized with an intraperitoneal injection of 50 mg/kg sodium pentobarbital. Bilateral ovaries of the mice in the OVX group were removed, while in the sham group, 1 g of adipose tissue surrounding bilateral ovaries (distance from ovaries, \sim 0.5 cm) was removed. After one month, a micro-CT was performed to validate the success of the model. Mice were sacrificed by cervical dislocation and 1 ml of blood was collected from the abdominal aorta of each mouse. For serum collection, blood was allowed to coagulate for 30 min at room temperature, followed by centrifugation at 2,000 \times g for 10 min at 4 $^{\circ}$ C. Serum estradiol levels were determined using a mouse estrogen ELISA kit (cat. no. KGE014; R&D Systems, Inc.), according to the manufacturer's protocol.

Flow cytometry. The mice from the OVX and sham group were sacrificed by cervical dislocation and soaked in ethanol for 5 min. Spleens were excised, mixed with Hanks' balanced salt solution (Gibco; Thermo Fisher Scientific, Inc.) and tissues were crushed through the mesh filter for mincing. Following washing with PBS and treatment with a Red Blood Cell Lysis buffer (cat. no. C3702; Beyotime Institute of Biotechnology), a total of 2 \times 10⁶ cells were suspended in flow tubes with 100 μ l of FACS staining buffer (2% FBS in PBS) and incubated with FITC conjugated anti-CD3 (1:200), APC-conjugated anti-CD4 (1:150), PE-conjugated anti-CD69 (1:100) and IgG isotype control (1:100) antibodies in the dark at 4 $^{\circ}$ C for 20 min. Following fixation in 2% formalin at room temperature for 20 min, cells were assessed using a FACScan Analyzer with FACSDiva software (version 6.2.1; BD Biosciences). Splenocytes were initially gated using forward and side scatter properties and CD4⁺ T cells were subsequently gated.

Isolation and culture of CD4⁺ T cells. Spleen single cell suspensions from the OVX and sham groups were incubated with magnetic beads coated with an anti-mouse CD4 antibodies. CD4⁺ T cells were isolated strictly according to the manufacturer's protocol. These purified cells were then subjected to RNA isolation in order to determine the expression levels of the proinflammatory cytokines IL-2, IFN- γ and TNF- α .

Purified T cells were maintained in RPMI-1640 medium (containing 10% FBS) at 37 $^{\circ}$ C with 5% CO₂ and seeded into a 12-well plate at a density of 1 \times 10⁵ cells/well. Following 24 h of culturing, the TNF- α level in the culture supernatant of T cells

was determined using a TNF- α ELISA kit, according to the manufacturer's protocol. The detection limit of this kit was 10.9-700 pg/ml.

T cells co-culture with BMMSCs. BMMSCs were isolated from the tibia and femur of mice, as previously described (27). Following three passages, BMMSCs were collected. The positive surface markers (CD29 and CD90) and the negative surface markers (CD34 and CD45) for BMMSCs (27,28) were analyzed by flow cytometry. MSCs were immunostained with FITC-conjugated antibodies against CD90 (cat. no. 11-0909-42; 1:20), CD45 (cat. no. 11-0451-82; 1:100), CD34 (cat. no. 11-0341-82; 1:100) and CD29 (cat. no. 11-0291-82; 1:50) at room temperature for 1 h. All antibodies were purchased from eBioscience, Thermo Fisher Scientific, Inc. Analysis was performed using a FACScan Analyzer and FACSDiva software (version 6.2.1; BD Biosciences) and the results demonstrated that the isolated BMMSCs were a relatively pure population of stromal cells that were negative for CD34 and CD45, and positive for CD29 and CD90 (Fig. S1). The single cell suspension from whole bone marrow was briefly cultured at 37°C with 5% CO₂ in α -MEM (containing 20% FBS). Following 24 h of culturing, the medium was replaced every 3 days after discarding the unattached cells and passaging was performed when cell confluence reached 80%.

A total of 2×10^6 CD4⁺ T cells from the sham group and OVX group were collected in cell culture plates, which were pre-coated with anti-CD3 (5 μ g/ml) antibodies for 4 h and anti-CD28 (2 μ g/ml) antibodies for 12 h, as previously described (28-30), and treated with anti-TNF- α (1 ng/ml) antibodies for 2 h at room temperature. At a concentration of 1×10^5 cells/well, T cells with anti-TNF- α antibody treatment or an equal volume of PBS from the sham group or OVX group were then transferred to 96-well culture plates pre-populated with BMMSCs (2×10^4 BMMSCs/well) and cultured for 7 days. The control group was the well that contained only BMMSCs.

MTT assay. A total of 1×10^3 /well T cells, with or without anti-TNF- α pretreatment, from the sham group and OVX group were added to BMMSC-coated wells (1.5×10^3 cells/well) in 96-well plates. At the indicated time (1, 2, 3, 4, 5, 6 or 7 days), 20 μ l of MTT solution (5 g/l) was added to each well. Following incubation for 4 h, the supernatant was discarded, 150 μ l of DMSO was added to each well and the solution was mixed for 10 min. OD values at 450 nm were determined using a Biotek Synergy H1 plate reader (BioTek Instruments, Inc.).

Cell cycle analysis. Cells were gathered and fixed with 70% ethanol at 4°C overnight. Cells were subsequently treated with ribonuclease A (20 μ g/ml; Sigma-Aldrich; Merck KGaA) and incubated with propidium iodide (50 μ g/ml; Sigma-Aldrich; Merck KGaA) for 30 min at 37°C. The population of cells in the G2-M, S and G0-G1 phases were determined using a FACScan Analyzer with FACSDiva software (version no. 6.2.1; BD Biosciences).

Alkaline phosphatase staining and Alizarin red staining assays. A total of 1×10^5 T cells with or without anti-TNF- α

treatment from the sham and OVX groups were co-cultured with 5×10^5 BMMSCs using osteogenic medium into 6-well plates. Following 7 days of culturing, the osteogenic medium was discarded. BMMSCs were washed twice with PBS and fixed with 4% paraformaldehyde at room temperature for 30 min. After being washed twice with PBS, the cells were treated with a BCIP/NBT solution in the dark for 30 min or stained with alizarin red staining solution for 30 min at 37°C.

Micro-CT detection. The distal femurs of mice were placed parallel to the long axis of the scanning bed, fixed with transparent tape and subjected to micro-CT scanning. The obtained microstructural imaging data were reconstructed and structural parameters, including bone volume/tissue volume (BV/TV), trabecula thickness, trabecula number and bone mineral density (BMD) were calculated using Inveon Research Workplace software (version no. 2.2; Siemens Healthineers).

RT-quantitative (RT-qPCR). Prior to extracting total RNA from bone fragments, collected bone tissues were placed in an RNase-free mortar with liquid nitrogen and ground into powder with a pestle. The obtained powders were then transferred into a tube containing TRIzol[®] (Invitrogen; Thermo Fisher Scientific, Inc.) and a Polytron[®] (Kinematic AG) homogenizer was used to further powder bone. Total RNA was isolated from bone fragments, CD4⁺ T cells or BMMSCs that had been co-cultured with T cells, both with and without anti-TNF- α , using TRIzol[®] (Invitrogen; Thermo Fisher Scientific, Inc.), according to the manufacturer's protocol. RT-qPCR was performed using the one-step RT-PCR kit, according to the manufacturer's protocol. RT-qPCR was conducted using the following thermocycling conditions: RT step at 55°C for 20 min; initial denaturation at 95°C for 5 min; 40 cycles of 95°C for 20 sec and 60°C for 1 min. The primers used in the current study were as follows: IL-2 forward, 5'-CCCAAGCAGGCCACAGAATTGAAA-3' and reverse, 5'-TGAGTCAAATCCAGAACATGCCGC-3'; IFN γ forward, 5'-TCAAGTGGCATAGATGTGGAAGAA-3' and reverse, 5'-TGGCTCTGCAGGATTTTCATG-3'; TNF- α forward, 5'-TCTTCTCATTCTGCTTGTGG-3' and reverse, 5'-GGTCTGGGCATAGAACTGA-3'; Runx2 forward, 5'-ATTGGCACCATCTTACTGTTACC-3' and reverse, 5'-CTCCTTAGAATCTGTTGCTCTCATA-3'; OCN forward, 5'-CTGACAAAGCCTTCATGTCCAA-3' and reverse, 5'-CCG CACGACAACCGCACCAT-3'; and β -actin forward, 5'-TGGCACCCAGCACAA TGAA-3' and reverse, 5'-CTAAGTCATAGTCCGCCTAGAAGCA-3'. Relative expression was calculated for each gene using the 2^{- $\Delta\Delta$ C_q} method (31) following normalization against β -actin expression. The methods used for measuring Runx2 and OCN mRNA expression from bone tissues were same as the methods for RT-qPCR using RNA from cells.

Western blotting. Following co-culturing for 7 days, BMMSCs were collected and assessed via western blotting. Cells were lysed in RIPA containing 1 mM phenylmethylsulfonyl fluoride (Beyotime Institute of Biotechnology). A Bradford protein assay (Bio-Rad Laboratories, Inc.) was used to quantify protein concentrations. Protein samples (25 μ g/well) were separated using 10% SDS-PAGE. Proteins were electrophoretically transferred onto PVDF membranes (0.45 mm; EMD Millipore).

Table I. The level of serum estradiol.

Group	Number	Serum estradiol (pg/ml)
Sham	10	48.88±17.89
OVX	10	10.44±3.80 ^a

^aP<0.05 vs. sham group. OVX, ovariectomized.

Following this, the membranes were blocked using 5% non-fat dry milk in TBS with 0.1% Tween-20 for 1 h at room temperature. The membranes were then incubated with anti-Runx2 (1:500), anti-OCN (1:500), anti-p-ERK (1:500), anti-ERK (1:500), anti-p-JNK (1:500), anti-JNK (1:500), anti-p-P38 (1:500), anti-P38 (1:500) and anti-β-actin (1:1,000) antibodies at 4°C overnight. This was followed by the incubation of membranes with horseradish peroxidase-conjugated secondary antibodies (1:5,000) at room temperature for 1 h. Membranes were visualized using an ECL system and protein expression levels were normalized to β-actin protein levels. The phosphorylated proteins were normalized to their corresponding total proteins.

Statistical analysis. Statistical analysis was performed using SPSS software (version no. 11.0; SPSS, Inc.). All data were expressed as mean ± standard deviation of ≥3 independent experiments. Unpaired Student's t-test or one-way ANOVA followed by a Tukey's post hoc test was used to analyze data. P<0.05 was considered to indicate a statistically significant difference.

Results

Bone formation and osteoblast differentiation is reduced in OVX mice. A month following resection, serum estradiol levels in the OVX group were significantly lower compared with the sham group (P<0.05; Table I). MicroCT images displayed significantly lower bone mass in the OVX group compared with the sham group (Fig. 1A and B). Furthermore, compared to the sham group, BV/TV, trabecular thickness, trabecular number and BMD were significantly reduced in the OVX group (P<0.05). These results indicated that the mouse PMO model, following ovarian ablation, was successfully constructed (Table II).

In order to assess osteoblast differentiation *in vivo*, the expression of markers of osteogenesis progression, Runx2 and OCN (32), in bone tissue was determined using RT-qPCR (Fig. 1C and D). Compared to the sham mice, lower levels of Runx2 and OCN were observed in the bone tissue of the OVX mice, indicating that osteoblast differentiation was reduced in OVX mice.

CD4⁺ T cells are activated in OVX mice. The proportions of CD4⁺CD69⁺ T cells in the spleen were analyzed using flow cytometry. CD4⁺ T cells were gated as demonstrated in Fig. 2A. In the OVX group, the spleen exhibited a significant increase in the proportion of CD4⁺CD69⁺T cells compared with the sham group (P<0.01; Fig. 2B). To further explore the

activation of T cells, the expression of proinflammatory cytokines in T cells was determined using RT-qPCR. The results indicated that the expression levels of IL-2, IFN-γ and TNF-α were all significantly higher (P<0.05) in T cells of the OVX group compared with the sham group (Fig. 2C).

ELISA results indicated that the expression of the pro-osteoclastogenic cytokine TNF-α in T lymphocytes of OVX mice was significantly higher compared with the sham group (Fig. 2D; P<0.05).

CD4⁺ T cells from OVX mice reduce BMMSC proliferation via TNF-α. To investigate the effects of CD4⁺ T cells on the proliferation of BMMSCs, MTT assays were performed (Fig. 3A). The results indicated that the proliferative ability of BMMSCs co-cultured with CD4⁺ T cells from OVX mice was significantly decreased compared with the sham group (P<0.05). However, this decreased proliferation ability was not observed in T cells that had received anti-TNF-α treatment (P<0.05). Furthermore, the cell cycle of BMMSCs was analyzed using flow cytometry and the results revealed that CD4⁺ T cells from OVX mice arrested the cell cycle of BMMSCs at the G2/M phase, an effect that was not observed in T cells that had received anti-TNF-α treatment (Fig. 3B).

TNF-α inhibits osteogenic differentiation of BMMSCs. In order to elucidate the effects of CD4⁺ T cells on BMMSCs osteogenic differentiation, alkaline phosphatase staining and alizarin red staining were performed. The results revealed that compared with the sham group, BMMSCs co-cultured with CD4⁺ T cells from OVX mice demonstrated less ALP activity and calcium deposition. Following T cell pre-treatment with anti-TNF-α, the ALP activity and calcium deposition levels were increased in BMMSCs co-cultured with CD4⁺ T cells from OVX mice, as well as in those from the sham group, compared to cells co-cultured with T cells that had not been pre-treated (Fig. 4A and B).

The osteoblastic differentiation of BMMSCs was further evaluated by examination of the expression of the osteoblastic markers Runx2 and OCN using RT-qPCR and western blotting (Fig. 4C and D). The results indicated that compared to the sham group, the expression of Runx2 and OCN were significantly decreased in BMMSCs co-cultured with CD4⁺ T cells from the OVX group (P<0.01). The expression levels of Runx2 and OCN were increased in BMMSCs co-cultured with CD4⁺ T cells from OVX mice that had been pretreated with anti-TNF-α (P <0.01), as well as in those in the sham group compared with BMMSCs co-cultured with cells that had not been pretreated (P<0.05).

Influence of CD4⁺ T cells on osteogenesis-related signaling pathways. To examine which signaling pathways were involved in CD4⁺ T cells exhibited decreased BMMSCs osteogenic differentiation in OVX mice, 7 days post-co-culturing the ERK, JNK and p38 MAPK osteogenesis-related signaling pathways were assessed (Fig. 5). The results revealed that these signaling pathways were significantly suppressed in BMMSCs co-cultured with CD4⁺ T cells from the OVX group (P<0.01), whereas they were restored following anti-TNF-α treatment (P<0.01). In T cells that had received pre-treatment with anti-TNF-α,

Table II. Metaphyseal morphological parameters in sham and OVX group.

Group	BV/TV (%)	Tb.Th (mm)	Tb.N (1/mm)	BMD (mg/cm ³)
Sham	20.13±3.24	0.68±0.07	4.61±0.40	409.80±21.55
OVX	4.95±1.29 ^b	0.08±0.02 ^b	2.82±0.70 ^a	260.45±18.79 ^a

^aP<0.05 and ^bP<0.01 vs. sham group. OVX, ovariectomized; BV/TV, bone volume/tissue volume; Tb.Th, trabecular thickness; Tb.N, trabecular number; BMD, bone mineral density.

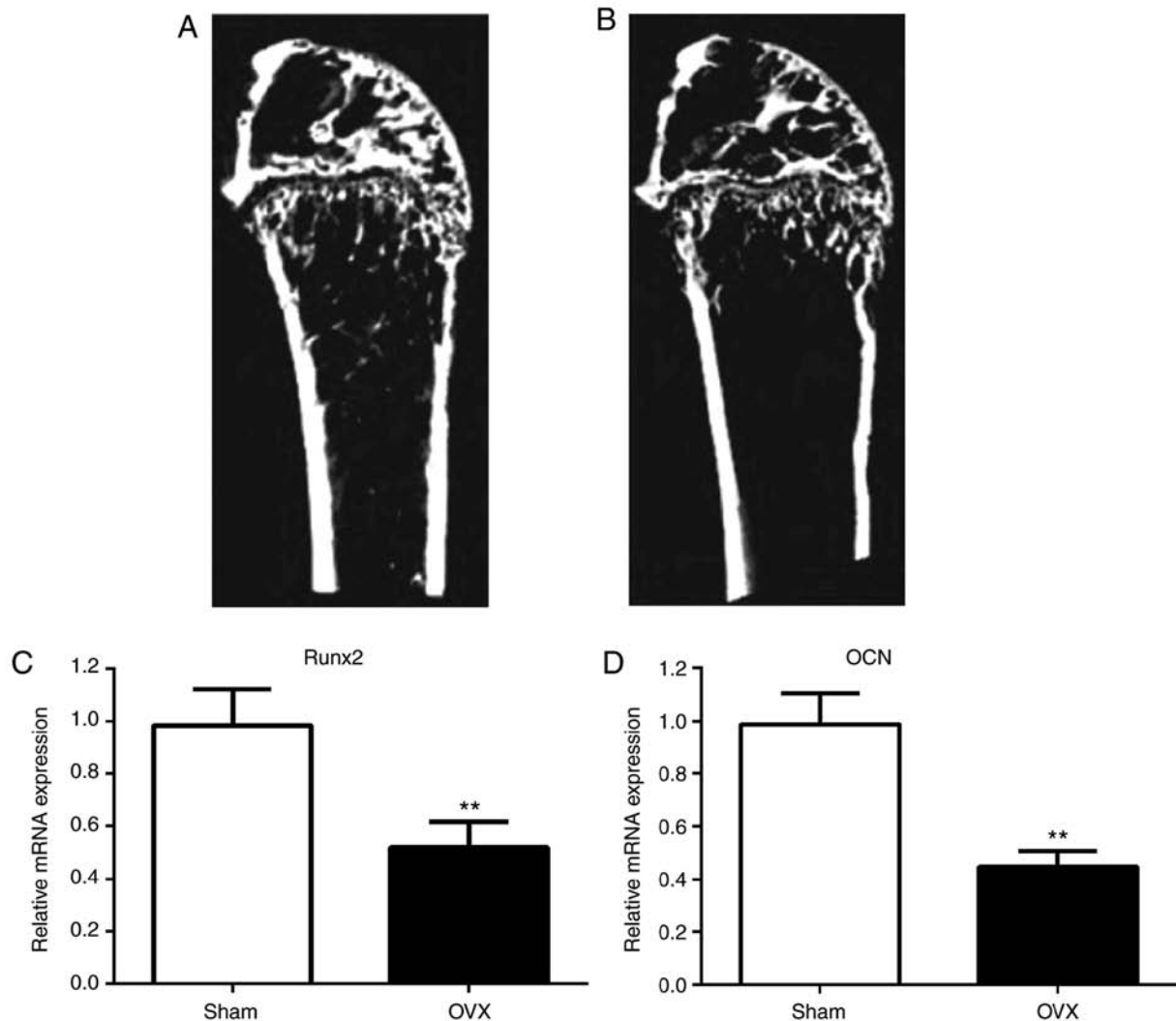


Figure 1. Bone formation and osteoblast differentiation is reduced in OVX mice. Micro-computer tomography reconstruction of distal femoral metaphyseal regions from mice in the (A) sham and (B) OVX groups. Reverse transcription-quantitative PCR analysis of (C) Runx-2 and (D) OCN mRNA levels in mouse bone tissues. **P<0.01 vs. sham. OVX, ovariectomized; Runx-2, runt related transcription factor 2; OCN, osteocalcin.

these three signaling pathways were further activated in BMMSCs co-cultured with CD4⁺ T cells from the sham group (P<0.01) compared with controls.

Discussion

In PMO, T cells have been identified as a critical cell population in promoting osteoclastogenesis (33). Moreover, as the principle source of osteogenic cells, the proliferation and osteogenic differentiation abilities of BMMSCs are

important factors to understand in order to develop improved osteoporosis treatments (34). The purpose of the present study was to investigate the effect of ovariectomy-induced CD4⁺ T cells on the proliferation and osteogenic differentiation of BMMSCs.

Previous studies have demonstrated that ovariectomy-induced osteoclastogenesis and bone loss are associated with increased T cell activation (35,36) and pro-osteoclastogenic cytokine TNF- α production (16,37). In the present study, the results indicated that the activation of CD4⁺ T cells was

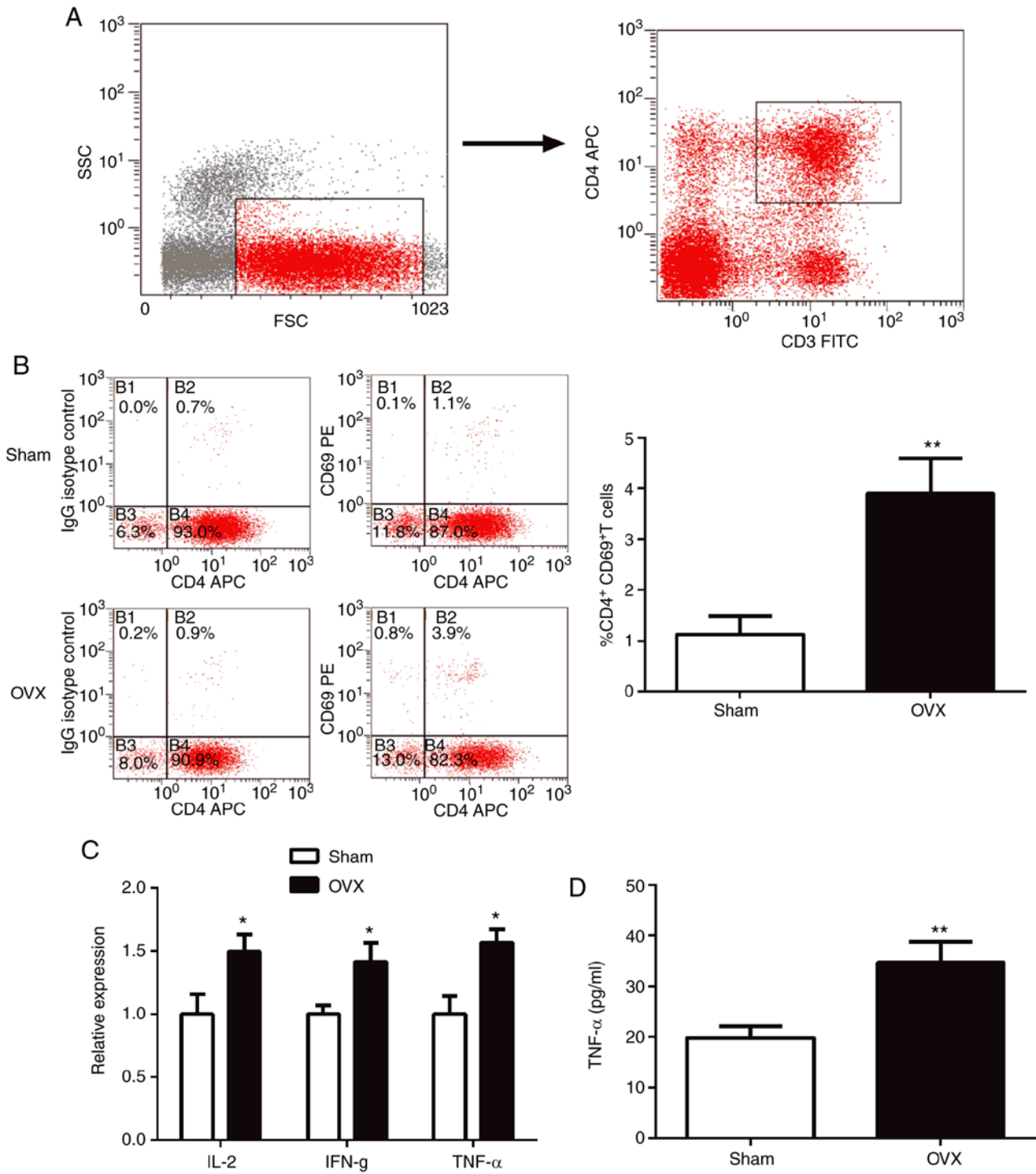


Figure 2. CD4⁺ T cells are activated in OVX mice. (A) The gating strategies used for CD4⁺ T cells. (B) Percentage of CD4⁺CD69⁺ cells in spleens tested using flow cytometry. (C) Expression levels of proinflammatory cytokines, IL-2, IFN- γ and TNF- α , in purified CD4⁺ T cells were determined using reverse transcription-quantitative-PCR. (D) TNF- α levels in the supernatant from purified CD4⁺ T cell cultures were measured by ELISA. *P<0.05, **P<0.01 vs. sham. CD, cluster of differentiation; OVX, ovariectomized; IL-2, interleukin 2; IFN- γ , interferon- γ ; TNF- α , tumor necrosis factor- α ; IgG, immunoglobulin; APC, allophycocyanin.

enhanced in OVX mice. This was determined by analyzing the percentage of CD4⁺CD69⁺ T cells in the spleen and the gene expression levels of the proinflammatory cytokines, IL-2, IFN- γ and TNF- α in CD4⁺ T cells isolated from OVX mice spleens. Furthermore, increased TNF- α levels were observed in cultured supernatants of CD4⁺ T cells isolated from OVX mice spleens.

In order to assess whether CD4⁺ T cells had an impact on the proliferation and osteogenic differentiation of BMMSCs, BMMSCs were co-cultured with CD4⁺ T cells from the OVX or sham group. A decrease in BMMSC proliferation ability was induced using CD4⁺ T cells from OVX mice. CD4⁺ T cells from OVX mice were also revealed to arrest the cell cycle of BMMSCs at the G2/M

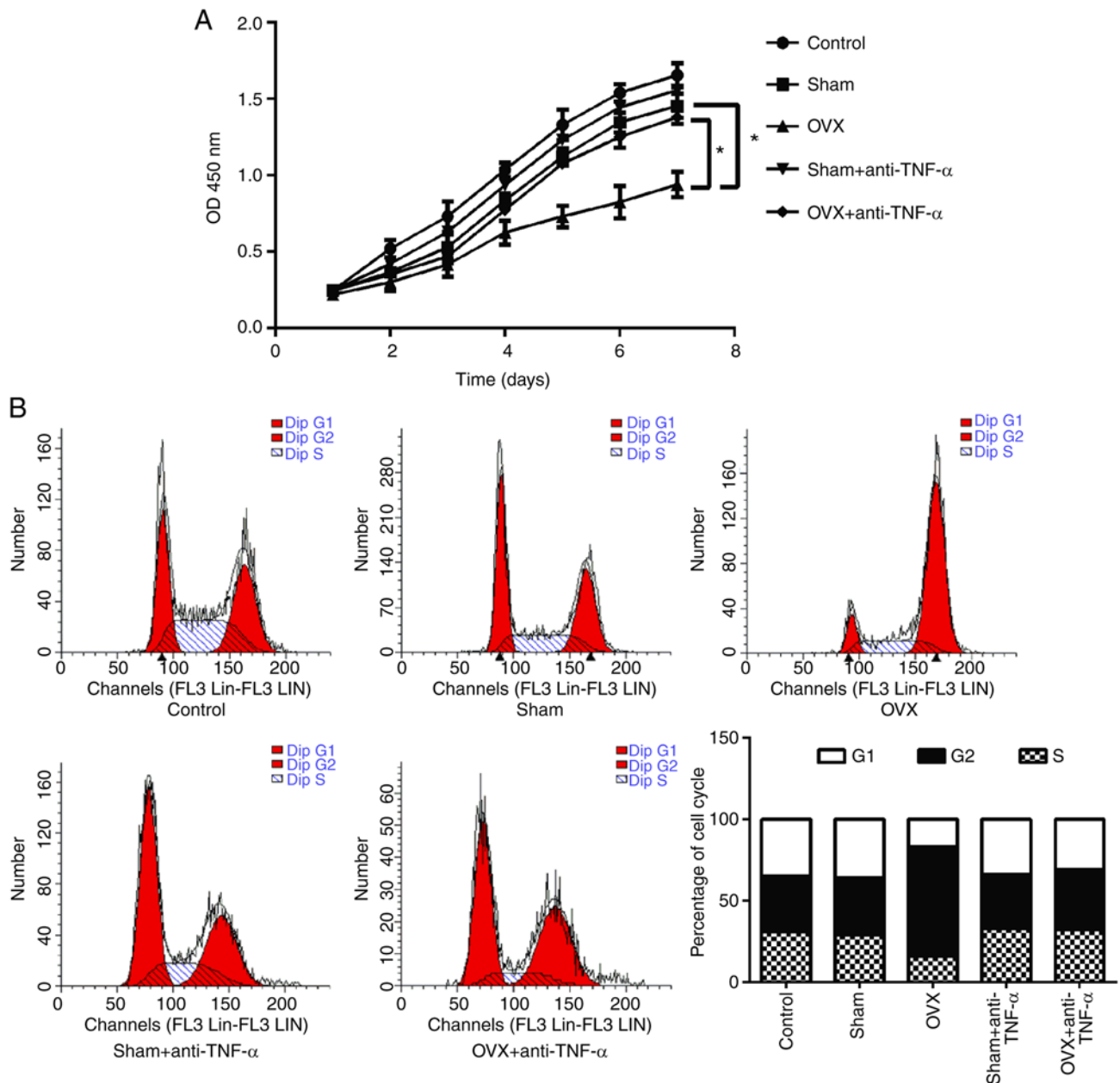


Figure 3. Effect of CD4⁺ T cells on the proliferation of BMMSCs. CD4⁺ T cells with or without anti-TNF- α treatment from the sham group and the OVX group were co-cultured with BMMSCs in osteogenic medium. (A) The proliferative ability of BMMSCs was detected by MTT at the indicated time points. *P<0.05 vs. the sham group at day 7. (B) Following 7 days of culturing, the cell cycle of BMMSCs was analyzed using flow cytometry. CD, cluster of differentiation; BMMSCs, bone marrow mesenchymal stem cells; TNF- α , tumor necrosis factor- α ; OVX, ovariectomized.

phase. Similarly, the osteogenic potential of BMMSCs was reduced using CD4⁺ T cells from the OVX group and demonstrated lower ALP activity, less calcium deposition and reduced expression of the osteoblastic marker genes, Runx2 and OCN.

Regarding the importance of TNF- α in ovariectomy-induced osteoclastogenesis, it was hypothesized that TNF- α secreted by activated CD4⁺ T cells mediated the inhibition of proliferation and osteogenic differentiation of BMMSCs. Following pre-treatment with CD4⁺ T cells with anti-TNF- α , the proliferation and osteogenic differentiation abilities of BMMSCs were fully restored. It has been confirmed by numerous studies that TNF- α stimulates the production of osteoclasts (38-40); however, the effects of TNF- α on stem

cell proliferation and osteogenic differentiation are still being explored. Recently, TNF- α has been reported to suppress the osteogenic differentiation of MSCs (41). The results from the present study indicated that CD4⁺ T cells inhibited the proliferation and osteogenic differentiation of BMMSCs by producing high levels of TNF- α .

There are a number of common crossover mechanisms between the immune response and bone remodeling. In the case of inflammation or injury, immune cells receive transmission information to act on osteoblasts and osteoclasts (42). Similarly, BMMSCs have an impact on T cells (43). Studies have found that BMMSCs affect the proliferation and differentiation of T cells through the use of exocrine and paracrine cytokines (44,45). The present study demonstrated

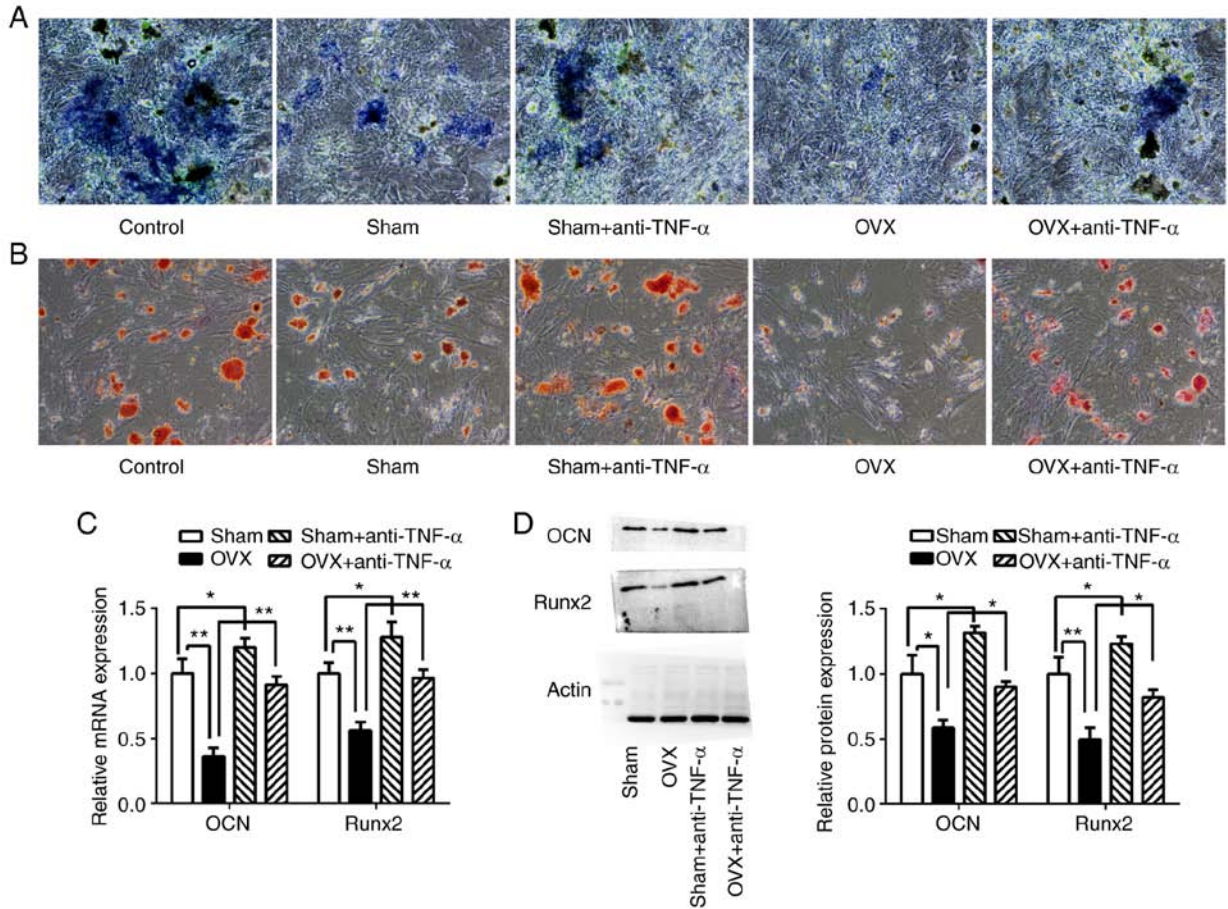


Figure 4. CD4⁺ T cells from OVX mice inhibited BMMSC osteogenic differentiation. CD4⁺ T cells with or without anti-TNF- α treatment from the sham group and the OVX group were co-cultured with BMMSCs in osteogenic medium. Following 7 days of culturing, (A) ALP staining and (B) Alizarin red staining were performed. (C) Relative mRNA expression of osteogenic marker genes in BMMSCs, Runx2 and OCN, were determined using reverse transcription-quantitative PCR. (D) Western blotting of Runx2 and OCN. *P<0.05. **P<0.01. CD, cluster of differentiation; OVX, ovariectomized; BMMSCs, bone marrow mesenchymal stem cells; TNF- α , tumor necrosis factor- α ; ALP, alkaline phosphatase; BMMSCs, bone marrow mesenchymal stem cells; Runx-2, runt related transcription factor 2; OCN, osteocalcin.

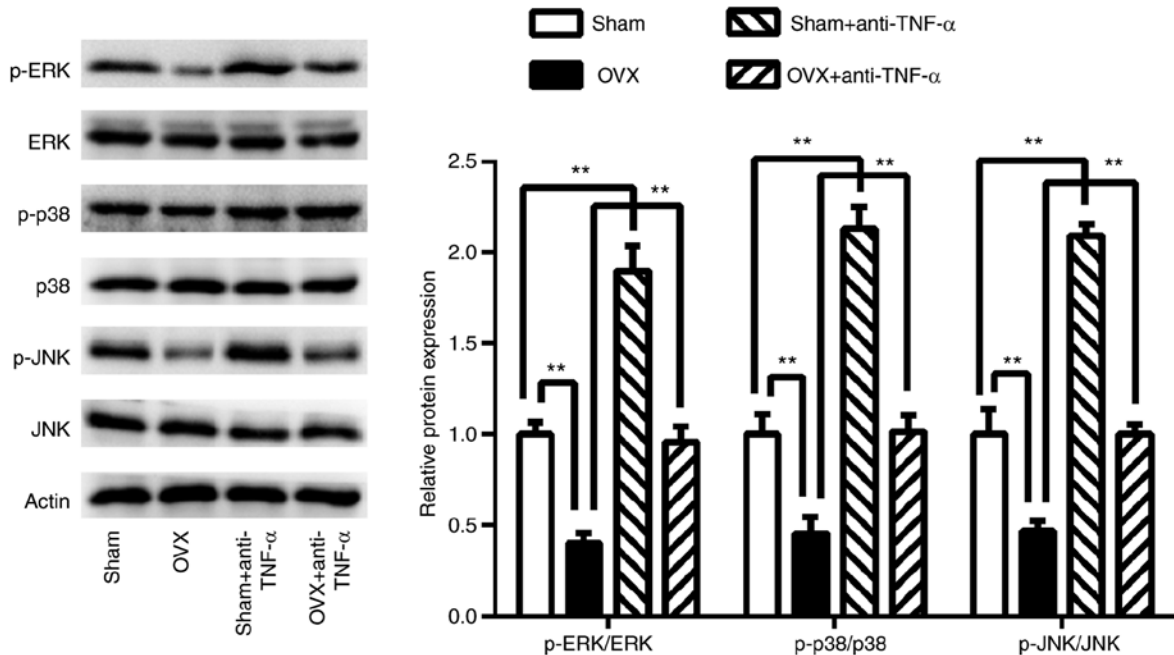


Figure 5. Influence of CD4⁺ T cells on osteogenesis-related signaling pathways. Following 7 days of co-culturing, the levels of p-ERK, p-p38 and p-JNK in bone marrow mesenchymal stem cells were determined via western blotting. **P<0.01. CD, cluster of differentiation; p, phosphorylated; ERK, extracellular signal-regulated kinase; JNK, c-Jun N-terminal kinase; OVX, ovariectomized; TNF- α , tumor necrosis factor- α .

that T cells also affected the proliferation and osteogenic differentiation of BMMSCs.

Previous studies have indicated that several MAPKs are essential components of the signal transduction machinery, which serve an important role in the differentiation process (46-48). Several MAPKs, including ERKs, JNK and p38 MAPK have been confirmed to be involved in the differentiation of MSCs into osteoblasts (41,49). In the present study, these signaling pathways were revealed to be critical for the osteogenesis of BMMSCs. CD4⁺ T cells from OVX mice inhibited the ERK, JNK and MAPK p38 signaling pathways, which suppressed the osteogenic differentiation of BMMSCs. Furthermore, this inhibition was remedied with an anti-TNF- α treatment.

As numerous studies have confirmed that the OVX-BMMSC have decreased proliferative ability and osteogenic differentiation in comparison to those from control animals (50-52), the phenotypes of BMMSC from OVX mice in the present study were not assessed. Furthermore, evaluating the effects of activated T cells on OVX-BMMSC would be challenging due to the reduced abilities of proliferation and osteogenic differentiation in OVX-BMMSC. In future studies, the influence of OVX-BMMSC on T cells will be evaluated, which will provide information about the underlying mechanisms between the immune response and bone remodeling in PMO.

In conclusion, to the best of our knowledge, the present study is the first to indicate that CD4⁺ T cells inhibit the proliferation and osteogenic differentiation of BMMSCs during the pathogenesis of OVX-induced osteoporosis and that this inhibition may be, at least partially, mediated via the enhanced expression of TNF- α by CD4⁺ T cells. These results may provide novel insight into the dysfunction of BMMSCs caused by estrogen deficiency.

Acknowledgements

Not applicable.

Funding

The present study was supported by the Medical Scientific Research Project of Chongqing Health Bureau (grant no. 2012-2-129), the National Natural Science Foundation of China (grant no. 81700958), the National Natural Science Foundation of China (grant no. 81800979) and the Science and Technology Project of Yubei District, Chongqing [grant no. 2017 (agriculture society) 45].

Availability of data and materials

The datasets used and/or analyzed during the current study are available from the corresponding author on reasonable request.

Authors' contributions

BYS, NG and WMH conceived and designed the experiments. BYS and LW conducted the experiments. BYS, YY, LC and WMH performed data analysis, interpretation and discussion. BYS wrote the manuscript. LW, NG and WMH revised the manuscript. All authors read and approved the final manuscript.

Ethics approval and consent to participate

Animal studies were approved by the Ethics Committee of Chongqing Medical University (Chongqing, China; approval no. 2018101702).

Patient consent for publication

Not applicable.

Competing interests

The authors declare that they have no competing interests.

References

- Lane JM, Russell L and Khan SN: Osteoporosis. *Clin Orthop Relat Res* 139-150, 2000.
- McCormick RK: Osteoporosis: Integrating biomarkers and other diagnostic correlates into the management of bone fragility. *Altern Med Rev* 12: 113-145, 2007.
- De Martinis M, Sirufo MM and Ginaldi L: Osteoporosis: Current and emerging therapies targeted to immunological checkpoints. *Curr Med Chem*: Jul 30, 2019 (Epub ahead of print). doi: 10.2174/0929867326666190730113123.
- Aggarwal BB, Shishodia S, Takada Y, Banerjee S, Newman RA, Bueso-Ramos CE and Price JE: Curcumin suppresses the paclitaxel-induced nuclear factor-kappaB pathway in breast cancer cells and inhibits lung metastasis of human breast cancer in nude mice. *Clin Cancer Res* 11: 7490-7498, 2005.
- Datta HK, Ng WF, Walker JA, Tuck SP and Varanasi SS: The cell biology of bone metabolism. *J Clin Pathol* 61: 577-587, 2008.
- Khosla S, Oursler MJ and Monroe DG: Estrogen and the skeleton. *Trends Endocrinol Metab* 23: 576-581, 2012.
- Adori M, Kiss E, Barad Z, Barabás K, Kiszely E, Schneider A, Kövesdi D, Sziksz E, Abrahám IM, Matkó J and Sármay G: Estrogen augments the T cell-dependent but not the T-independent immune response. *Cell Mol Life Sci* 67: 1661-1674, 2010.
- Zhang N, Gui Y, Qiu X, Tang W, Li L, Gober HJ, Li D and Wang L: DHEA prevents bone loss by suppressing the expansion of CD4(+) T cells and TNF α production in the OVX-mouse model for postmenopausal osteoporosis. *Biosci Trends* 10: 277-287, 2016.
- Faienza MF, Ventura A, Marzano F and Cavallo L: Postmenopausal osteoporosis: The role of immune system cells. *Clin Dev Immunol* 2013: 575936, 2013.
- Eastell R, O'Neill TW, Hofbauer LC, Langdahl B, Reid IR, Gold DT and Cummings SR: Postmenopausal osteoporosis. *Nat Rev Dis Primers* 2: 16069, 2016.
- Li JY, Tawfeek H, Bedi B, Yang X, Adams J, Gao KY, Zayzafoon M, Weitzmann MN and Pacifici R: Ovariectomy deregulates osteoblast and osteoclast formation through the T-cell receptor CD40 ligand. *Proc Natl Acad Sci USA* 108: 768-773, 2011.
- Song H, Li X, Zhao Z, Qian J, Wang Y, Cui J, Weng W, Cao L, Chen X, Hu Y and Su J: Reversal of osteoporotic activity by endothelial cell-secreted bone targeting and biocompatible exosomes. *Nano Lett* 19: 3040-3048, 2019.
- Chen X, Zhi X, Wang J and Su J: RANKL signaling in bone marrow mesenchymal stem cells negatively regulates osteoblastic bone formation. *Bone Res* 6: 34, 2018.
- Uehara IA, Soldi LR and Silva MJB: Current perspectives of osteoclastogenesis through estrogen modulated immune cell cytokines. *Life Sci* 256: 117921, 2020.
- Sang C, Zhang J, Zhang Y, Chen F, Cao X and Guo L: TNF- α promotes osteoclastogenesis through JNK signaling-dependent induction of Semaphorin3D expression in estrogen-deficiency induced osteoporosis. *J Cell Physiol* 232: 3396-3408, 2017.
- Roggia C, Gao Y, Cenci S, Weitzmann MN, Toraldo G, Isaia G and Pacifici R: Up-regulation of TNF-producing T cells in the bone marrow: A key mechanism by which estrogen deficiency induces bone loss in vivo. *Proc Natl Acad Sci USA* 98: 13960-13965, 2001.
- Li J, Wang Q, Yang R, Zhang J, Li X, Zhou X and Miao D: BMI-1 mediates estrogen-deficiency-induced bone loss by inhibiting reactive oxygen species accumulation and T cell activation. *J Bone Miner Res* 32: 962-973, 2017.

18. Bi H, Ming L, Cheng R, Luo H, Zhang Y and Jin Y: Liver extracellular matrix promotes BM-MSCs hepatic differentiation and reversal of liver fibrosis through activation of integrin pathway. *J Tissue Eng Regen Med* 11: 2685-2698, 2017.
19. Phinney DG: Biochemical heterogeneity of mesenchymal stem cell populations: Clues to their therapeutic efficacy. *Cell Cycle* 6: 2884-2889, 2007.
20. Bi H and Jin Y: Current progress of skin tissue engineering: Seed cells, bioscaffolds, and construction strategies. *Burns Trauma* 1: 63-72, 2013.
21. Kim KI, Park S and Im GI: Osteogenic differentiation and angiogenesis with cocultured adipose-derived stromal cells and bone marrow stromal cells. *Biomaterials* 35: 4792-4804, 2014.
22. Pilz GA, Ulrich C, Ruh M, Abele H, Schäfer R, Kluba T, Bühring HJ, Roluffs B and Aicher WK: Human term placenta-derived mesenchymal stromal cells are less prone to osteogenic differentiation than bone marrow-derived mesenchymal stromal cells. *Stem Cells Dev* 20: 635-646, 2011.
23. Gimble JM and Nuttall ME: The relationship between adipose tissue and bone metabolism. *Clin Biochem* 45: 874-879, 2012.
24. Singh A, Mehdi AA, Srivastava RN and Verma NS: Immunoregulation of bone remodelling. *Int J Crit Illn Inj Sci* 2: 75-81, 2012.
25. Liu Y, Wang L, Kikuri T, Akiyama K, Chen C, Xu X, Yang R, Chen W, Wang S and Shi S: Mesenchymal stem cell-based tissue regeneration is governed by recipient T lymphocytes via IFN- γ and TNF- α . *Nat Med* 17: 1594-1601, 2011.
26. Martinet L, Fleury-Cappellesso S, Gadelorge M, Dietrich G, Bourin P, Fournié JJ and Poupor R: A regulatory cross-talk between Vgamma9Vdelta2 T lymphocytes and mesenchymal stem cells. *Eur J Immunol* 39: 752-762, 2009.
27. Biver G, Wang N, Gartland A, Orriss I, Arnett TR, Boeynaems JM and Robaye B: Role of the P2Y13 receptor in the differentiation of bone marrow stromal cells into osteoblasts and adipocytes. *Stem Cells* 31: 2747-2758, 2013.
28. Yamaza T, Miura Y, Bi Y, Liu Y, Akiyama K, Sonoyama W, Patel V, Gutkind S, Young M, Gronthos S, *et al*: Pharmacologic stem cell based intervention as a new approach to osteoporosis treatment in rodents. *PLoS One* 3: e2615, 2008.
29. Eljaafari A, Tartelin ML, Aissaoui H, Chevrel G, Osta B, Lavocat F and Miossec P: Bone marrow-derived and synovium-derived mesenchymal cells promote Th17 cell expansion and activation through caspase 1 activation: Contribution to the chronicity of rheumatoid arthritis. *Arthritis Rheum* 64: 2147-2157, 2012.
30. Duffy MM, Pindjakova J, Hanley SA, McCarthy C, Weidhofer GA, Sweeney EM, English K, Shaw G, Murphy JM, Barry FP, *et al*: Mesenchymal stem cell inhibition of T-helper 17 cell-differentiation is triggered by cell-cell contact and mediated by prostaglandin E2 via the EP4 receptor. *Eur J Immunol* 41: 2840-2851, 2011.
31. Livak KJ and Schmittgen TD: Analysis of relative gene expression data using real-time quantitative PCR and the 2(-Delta Delta C(T)) Method. *Methods* 25: 402-408, 2001.
32. Duan L, Zhao H, Xiong Y, Tang X, Yang Y, Hu Z, Li C, Chen S and Yu X: miR-16-2^{*} Interferes with WNT5A to Regulate Osteogenesis of Mesenchymal Stem Cells. *Cell Physiol Biochem* 51: 1087-1102, 2018.
33. Kelleher FC and O'Sullivan H: Monocytes, macrophages, and osteoclasts in osteosarcoma. *J Adolesc Young Adult Oncol* 6: 396-405, 2017.
34. Kang SK, Shin IS, Ko MS, Jo JY and Ra JC: Journey of mesenchymal stem cells for homing: Strategies to enhance efficacy and safety of stem cell therapy. *Stem Cells Int* 2012: 342968, 2012.
35. D'Amelio P, Grimaldi A, Di Bella S, Brianza SZM, Cristofaro MA, Tamone C, Giribaldi G, Ulliers D, Pescarmona GP and Isaia G: Estrogen deficiency increases osteoclastogenesis up-regulating T cells activity: A key mechanism in osteoporosis. *Bone* 43: 92-100, 2008.
36. Zhang JL, Qiu XM, Zhang N, Tang W, Gober HJ, Li DJ and Wang L: BuShenNingXin decoction suppresses osteoclastogenesis by modulating RANKL/OPG imbalance in the CD4⁺ T lymphocytes of ovariectomized mice. *Int J Mol Med* 42: 299-308, 2018.
37. Aoki K, Saito H, Itzstein C, Ishiguro M, Shibata T, Blaque R, Mian AH, Takahashi M, Suzuki Y, Yoshimatsu M, *et al*: A TNF receptor loop peptide mimic blocks RANK ligand-induced signaling, bone resorption, and bone loss. *J Clin Invest* 116: 1525-1534, 2006.
38. Kudo O, Fujikawa Y, Itonaga I, Sabokbar A, Torisu T and Athanasou NA: Proinflammatory cytokine (TNF α /IL-1 α) induction of human osteoclast formation. *J Pathol* 198: 220-227, 2002.
39. Algate K, Haynes DR, Bartold PM, Crotti TN and Cantley MD: The effects of tumour necrosis factor- α on bone cells involved in periodontal alveolar bone loss; osteoclasts, osteoblasts and osteocytes. *J Periodont Res* 51: 549-566, 2016.
40. Marahleh A, Kitaura H, Ohori F, Kishikawa A, Ogawa S, Shen WR, Qi J, Noguchi T, Nara Y and Mizoguchi I: TNF- α Directly Enhances Osteocyte RANKL Expression and Promotes Osteoclast Formation. *Front Immunol* 10: 2925, 2019.
41. Du D, Zhou Z, Zhu L, Hu X, Lu J, Shi C, Chen F and Chen A: TNF- α suppresses osteogenic differentiation of MSCs by accelerating P2Y2 receptor in estrogen-deficiency induced osteoporosis. *Bone* 117: 161-170, 2018.
42. Kumar G and Roger PM: From Crosstalk between Immune and Bone Cells to Bone Erosion in Infection. *Int J Mol Sci* 20: 5154, 2019.
43. Lecarpentier Y, Schussler O, Sakic A, Rincon-Garriz JM, Soulie P, Bochaton-Piallat ML and Kindler V: Human bone marrow contains mesenchymal stromal stem cells that differentiate in vitro into contractile myofibroblasts controlling t lymphocyte proliferation. *Stem Cells Int* 2018: 6134787, 2018.
44. Lu X, Wang X, Nian H, Yang D and Wei R: Mesenchymal stem cells for treating autoimmune dacryoadenitis. *Stem Cell Res Ther* 8: 126, 2017.
45. Rios C, Garbayo E, Gomez LA, Curtis K, D'Ippolito G and Schiller PC: Stem cells and their contribution to tissue repair. *Stem Cell Regenerative Medicine* 1: 9-22, 2010.
46. Sun Y, Liu WZ, Liu T, Feng X, Yang N and Zhou HF: Signaling pathway of MAPK/ERK in cell proliferation, differentiation, migration, senescence and apoptosis. *J Recept Signal Transduct Re* 35: 600-604, 2015.
47. Cai TY, Zhu W, Chen XS, Zhou SY, Jia LS and Sun YQ: Fibroblast growth factor 2 induces mesenchymal stem cells to differentiate into tenocytes through the MAPK pathway. *Mol Med Rep* 8: 1323-1328, 2013.
48. Hwang JH, Byun MR, Kim AR, Kim KM, Cho HJ, Lee YH, Kim J, Jeong MG, Hwang ES and Hong JH: Extracellular Matrix Stiffness Regulates Osteogenic Differentiation through MAPK Activation. *PLoS One* 10: e0135519, 2015.
49. Huang RL, Yuan Y, Tu J, Zou GM and Li Q: Opposing TNF- α /IL-1 β - and BMP-2-activated MAPK signaling pathways converge on Runx2 to regulate BMP-2-induced osteoblastic differentiation. *Cell Death Dis* 5: e1187, 2014.
50. Zhou S, Zilberman Y, Wassermann K, Bain SD, Sadovsky Y and Gazit D: Estrogen modulates estrogen receptor alpha and beta expression, osteogenic activity, and apoptosis in mesenchymal stem cells (MSCs) of osteoporotic mice. *J Cell Biochem Suppl* 36: 144-155, 2001.
51. Yang N, Wang G, Hu C, Shi Y, Liao L, Shi S, Cai Y, Cheng S, Wang X, Liu Y, *et al*: Tumor necrosis factor alpha suppresses the mesenchymal stem cell osteogenesis promoter miR-21 in estrogen deficiency-induced osteoporosis. *J Bone Miner Res* 28: 559-573, 2013.
52. Sang C, Zhang Y, Chen F, Huang P, Qi J, Wang P, Zhou Q, Kang H, Cao X and Guo L: Tumor necrosis factor alpha suppresses osteogenic differentiation of MSCs by inhibiting semaphorin 3B via Wnt/ β -catenin signaling in estrogen-deficiency induced osteoporosis. *Bone* 84: 78-87, 2016.



This work is licensed under a Creative Commons Attribution-NonCommercial-NoDerivatives 4.0 International (CC BY-NC-ND 4.0) License.